Physical modeling of the vibration mitigation by an isolating screen

Modélisation physique de l'atténuation des vibrations par un écran isolant

Masoumi H., Vanhonacker P.
D2S international, Leuven, Belgium

ABSTRACT: The vibrations generated by railway traffic in urban area can be mitigated using the isolating screens. Both experimental and numerical simulations have been used by authors to realize the vibration transmission through the ground and the soil-barrier interaction. Since a full-scale test is usually expensive and has some difficulties and limitations in terms of the soil conditions and the cost of screen construction, a physical modeling of the problem in small-scale has been proposed. In frame of an European project, a test bench consisting of a soil container and an isolating screen has been fabricated. The container is filled with a very fine sand using the pluviation technique to guarantee the uniformity of the soil conditions and the repeatability of the test. A small foundation excited by a shaker at different frequency ranges is used as the vibration source. The soil responses are measured by accelerometers placed on the soil surface at different distances from the source. The isolating efficiency of a concrete screen has been examined. Results of experimental measurements show a reasonable agreement with those obtained by the numerical modeling.

RÉSUMÉ : Les vibrations générées par le trafic ferroviaire dans les zones urbaines peuvent être atténuées par un écran antivibratoire. Les simulations expérimentales ou numériques ont été utilisées par les auteurs pour réaliser la transmission des vibrations par le sol ainsi que l'interaction sol-écran. Tandis qu'un essai à grande échelle est généralement cher et difficile à réaliser en termes de conditions du sol et de coût de construction, une modélisation physique du problème en échelle réduite a été proposée. Dans la cadre d'un projet européen, un banc d'essai constitué d'un conteneur de sol et un écran isolant a été fabriqué. Le conteneur est rempli par un sable très fin en utilisant la technique de pluviation afin de garantir l'uniformité des conditions du sol et la répétabilité de l'essai. Une petite fondation excitée par un excitateur à différentes gammes de fréquences a été utilisée comme source de vibrations. Les réponses du sol sont mesurées par des accéléromètres placés sur la surface du sol à différentes distances de la source. L'efficacité d'isolation d'un écran en béton a été examinée. Les résultats des mesures expérimentales montrent un accord raisonnable avec ceux obtenus par la modélisation numérique.

KEYWORDS: Small-scale test, pluviation, soil-structure interaction, vibration mitigation, isolating screen.

1 INTRODUCTION

To assess the efficiency of isolating screens, besides several numerical computations presented and discussed in the literature (Adam and von Estorff 2005 , François et al. 2010), a few researchers have been focused on experimental tests (Celebi et al. 2010). Since a full-scale test is usually expensive and has some difficulties and limitations in terms of the soil conditions and isolating screen construction, small-scale tests with their flexibility for selecting different soil conditions and screen properties are more relevant. A major difficulty facing the physical modeling of vibration problems in the soil is the repeatability of the test and the replication of the in-situ stress field. Other difficulties for realizing the boundary conditions in the infinity where there are no reflections, may be resolved by selecting an appropriate scale factor or a relevant size for the soil container.

The similarity of the conditions between the model (small-scale) and the prototype (full-scale) is guaranteed by the scaling factors. The scaling factor is defined to extrapolate the relation between the results of the small-scale testing to those of the prototype. These relations represent the effects of the geometric and the stress scale. Three different scale factors between the small-scale model and the prototype can be defined as follows (Altaee and Fellenius 1994), where the subscripts "m" and "p" denote to the model and the prototype, respectively:

(1) the geometric scale ratio $N = L_p/L_m$, that represents a linear relation between the corresponding dimensions in the full-scale prototype and the small-scale model,

(2) the effective stress scale ratio $n = \sigma'_p/\sigma'_m$, that represents the ratio of the effective stress at a certain depth in the prototype to that at the corresponding depth in the model,

(3) the effective stress gradient ratio $I = \dot{\sigma}'_p/\dot{\sigma}'_m$, that is the rate of change of stress with depth to that of the prototype. In a conventional physical testing, and for the normal gravity condition (1g model), the product of the stress-gradient ratio (I) and the geometric scale ratio (N) is equal to unity when n = 1. However, in a dry soil, the effective stress is equal to γz, and the scaling factor n is related to the geometrical scaling factor N such that $n = N(\gamma_p/\gamma_m)$, where γ_p and γ_m are the unit weights of the soil in the prototype and the model.

In a wave propagation problem (as a dynamic problem), an additional scaling factor should also be considered for the time or the frequency to guarantee the similarity of the stress wave transmissibility in the model and the prototype. In a low strain dynamic problem (a linear problem) where the influence of the soil stress condition in the soil behavior can be neglected, the dimensionless frequency ratio ($\omega L/C$) must be identical in both small and full scale test, where ω is the excitation frequency, and C is the wave velocity. Therefore, it can be written that

$$(\omega L/C)_p = (\omega L/C)_m \quad (1)$$

This results in the frequency scaling factor $\omega_p/\omega_m = (C_p/C_m)/N$, and for identical wave velocity in model and in the prototype, the frequency scaling factor is equal to the inverse of the geometrical factor N. In table 1, the prototype to model ratio's for different physical units are presented where identical soil properties (E, ρ, ν) in both model and prototype are assumed. E, ρ, and ν are the Young's modulus, the density and the Poisson's ratio, respectively.

Table 1. Scaling factor for different physical units.

Physical unit	Prototype/Model
Length W, H, R	N
Frequency	1/N
Time	N
Velocity	1
Acceleration	1/N
Wavelength	N
Dimensionless length W/λ, H/λ, R/λ	1

Since an unbounded half space soil medium is replaced by a container with limited dimensions, radiation conditions at the boundaries cannot be satisfied perfectly. It is well known that body and surface waves lose the most of their energy after traveling some cycles of motion or wavelengths through the soil (after 3 to 4 wavelength) because of the geometric and material damping. So appropriate container dimensions and the excitation frequency must be selected to reduce these effects. In principle, screen dimensions (width and length) are normalized with respect to the shear wavelength to be comparable at different frequencies.

2 TEST BENCH

The test bench consists of the following parts:
1) The container: a demountable box with a floor, and side walls. The walls are made by deformed galvanized-steel plates with 0.75 mm thickness. Interior of the container, side walls and the floor covered by wooden plates to provide a proper smooth surface.
2) The isolating screen: a concrete slab that can be covered by a thin layer of resilient material. The isolating screen is completely embedded in the soil medium.
3) The soil: a sieved, dried fine sand.

2.1 *The soil treatment*

The container is filled with Mol silica sand with an average grain size (D_{50}) of 0.26 mm. The sand is properly sieved, washed and then dried.
The soil treatment should be (1) repeatable, (2) operator-independent, and should results in (3) a tight tolerance in soil conditions (uniformity of the soil density).
Investigation in different soil deposition methods (Miura and Toki 1982, Vaid et al. 1999) have shown that the pluviation method is less operator-dependent and more repeatable than the other methods such as the moist tamping, dry tapping (the sand being poured in layers) and pouring using a hand rotated flask.
The density of pluviated specimen depends on (1) the fall height, (2) the depositional intensity, and (3) the uniformity of the sand raining. To provide a uniform density, it has been shown that the pluviation device should be raised continuously with a constant low fall height and a constant drop energy.
Since an universal device does not exist for the soil deposition by the pluviation, a pluviation device compatible with the container dimensions has been designed and fabricated. The pluviation device consists of three main parts:
1) A tank or reservoir in the upper level to deliver the sand through a nuzzle, 2) A shutter that can be in open/close position to control the deliverance of sand. Shutter consists of a fixed perforated plate and a sliding plate. Opening the sliding plate let the sand to pass through the holes in the perforated plate.
3) A diffuser consisting of a guide box with two grids (sieves). The second grid is posed at the lower part of device and its holes have different direction to polarize the drop.
The sand delivers from the top by its gravity through the opened-shutter. The minimum fall height can be modified by changing the position of the diffuser respect to the soil surface.

Figure 1. The sand deposition by the pluviation technique.

As the rate of the sand flow increases, because of the air turbulence, a non-flat surface of the sand is generated. This effect generally happens when the sand is raining with a high flow rate and higher fall height. The air turbulence and non-uniformity can be controlled by reducing the fall height as well as by decreasing the depositional intensity.
The sand deposition has been performed using the pluviation device that moves on two rails over the container with a speed of approximately 0.18 to 0.2 m/s. The height of the sand drop is varied from 15 to 20 cm, figure 1.

2.2 *Investigation on sand properties*

The sand density has been measured conventionally during pluviation by posing small cylindrical receptacles in different depth. To measure in-situ density, a total of 16 receptacles were installed at different depths: 40 cm, 20 cm and at the surface of the sand. The receptacles were distributed along the container width at distances of 40 cm and 60 cm from the container sidewalls. Results show an average density of 1640 kg/m3 near to the surface, 1685 kg/m3 at 20 cm in depth and 1700 kg/m3 at 40 cm in depth.
In addition, upon completion of the soil pluviation, the uniformity of the soil stiffness (at the top layer) is examined by the impedance test. The test configuration consists of a small steel foundation, two accelerometers installed on the foundation, and a hammer, figure 2.
The foundation response due to several hammer impacts is measured. A set of points on the sand surface has been selected for the impedance test.
Figure 3 shows the mobility function of the foundation measured due to the impact hammer test. Results show a resonance frequency range from 120 to 130 Hz at different measurement points.
Since the foundation is rigid, the dynamic foundation-soil system can be modeled with a dynamic system with a single degree of freedom with the foundation mass and the soil stiffness.

Figure 2. Impedance test using a hammer impact on the foundation.

So, the equation of motion of the system can be written as:

$$-m_f\omega^2 + i\omega C_z + K_z = \hat{F}(\omega) \quad (1)$$

, where K_z and C_z denote to the real and imaginary part of the vertical soil stiffness, and m_f is the mass of the foundation.

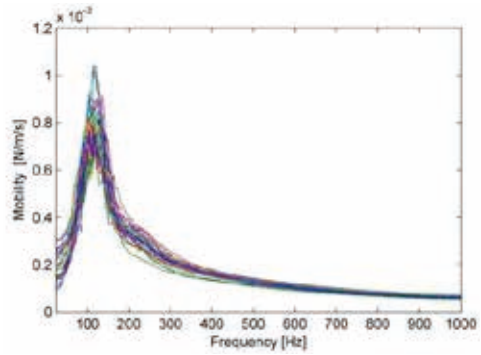

Figure 3. Mobility functions of the foundation.

At low dimensionless frequencies $a_0 = \omega r/C_s < 0.25$, the soil stiffness K_z is approximately equal to the static vertical impedance of a rigid foundation, underlying on a homogeneous half space, (Sieffert and Cevaer 1992):

$$K_z = 4G_s r/(1-\upsilon) \quad (2)$$

, where G_s is the shear modulus of the soil and r is the foundation ratio.

Using a curve-fitting technique based on the least-square method, each parameters of the equation of motion (1) can be identified. Therefore, the shear modulus of the upper layer of the sand can be determined. For r = 5 cm, ν= 0.33, the shear modulus in the center area of the container is almost uniformly distributed with an average value of 12.5 MPa. Near the sidewalls, however, the non-uniform distribution is observed.

The sand properties (the density and the shear modulus) measured by the density test and the impedance test will be used in the numerical modeling.

3 MEASUREMENT SETUP

The isolating screen is installed at the middle of the container. The screen is a concrete plate of 2.0 m x 0.4 m x 0.04 m. The measurement configuration consists of a small foundation posed on the soil surface where the dynamic force is applied and 10 accelerometers placed at the measurement points. The small foundation is excited at the frequency band of interest and the free field vibrations are measured symmetrically on both sides of the foundation, figure 4. This configuration enables us to simultaneously measure the non-isolated responses (on the side without the screen) and the isolated responses (on the side where the screen is installed).

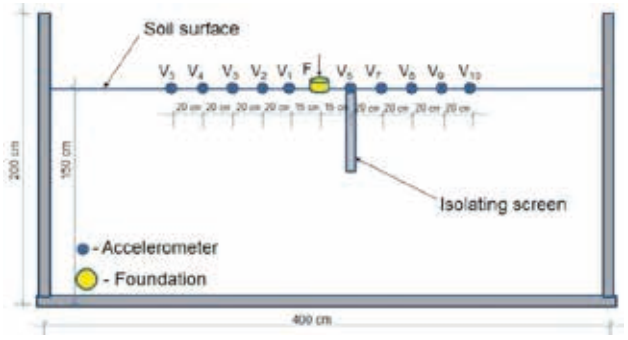

Figure 4. Overview of the measurement setup (the section view).

A shaker device is used for the excitation generation. The type, the amplitude and the frequency content of the excitation can be controlled by means of a wave generator software that feeds into a power amplifier, figure 5.

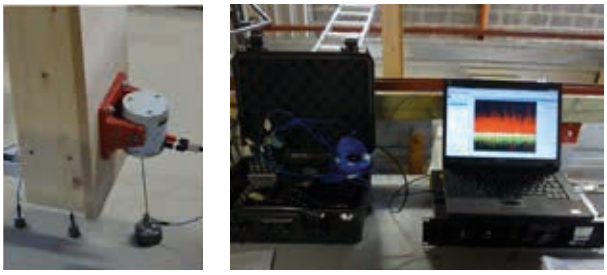

Figure 5. Shaker device and acquisition system.

A random vibration from 100 to 900 Hz is used. To obtain a reasonable coherency, the excitations were applied for a period of at least 3 minutes. Based on four frequency ranges, four separate measurements were performed.

Figure 6 shows the configuration of the measurements for the concrete barrier test. The efficiency of the isolating barrier is determined by introducing the insertion loss factor.

Figure 6. Measurement configuration for the concrete barrier test.

The insertion loss is defined using the peak particle velocity (PPV) obtained at each measurement points.

$$IL_{[dB]} = 20 \times \log_{10}\left(\frac{\mathrm{PPV_{isolated}}}{\mathrm{PPV_{non\text{-}isolated}}}\right) \quad (9)$$

, where the peak particle velocity (PPV) is defined as the maximum value of the impulse response function (IRF) at each measurement points.

Induced vibration due to railways traffic is mostly dominated in a frequency range from 10 to 60 Hz. According to the frequency range of interest and the dimension of the container, a geometrical scaling factor of 15 would be suitable.

A 2.5-dimensional coupled FE-BE method is used for modeling of the problem. In 2.5-dimensional modeling, a longitudinally invariant geometry of the structure (the barrier) is assumed.

In this methodology, 2.5D FEM is used to model the structure (the screen) and the soil impedance as well as the free field vibrations are computed by means of 2.5D BEM. This methodology has been already examined for different applications such as railway tracks, roads, tunnels, dams, trenches, and pipelines by François et al. (2010).

Table 3 Frequency ranges in the full scale and the small-scale test.

Small-scale test N=15	Full-scale test
100-300 [Hz]	6.7 – 20 [Hz]
300-500 [Hz]	20 - 33.3 [Hz]
500-700 [Hz]	33.3 - 46.7 [Hz]
700-900 [Hz]	46.7 – 60 [Hz]

The barrier has a width of 0.04*15 = 0.60 m and a depth of 0.4*15 = 6 m. Table 3 shows the frequency ranges that have been applied for the measurements.
The same soil properties as obtained in the test bench are considered. A soft layer over a homogeneous half space is considered. The soil characteristics are presented in table 4. The soil has a material damping of 5%.

Table 4 Soil properties in numerical modeling.

Layer depth	Young's modulus	Density	Shear wave velocity
3 [m]	33.5 [MPa]	1660 kg/m³	85 [m/s]
∞	65 [MPa]	1690 kg/m³	120 [m/s]

Figure 7 shows the variation of the insertion loss versus the distance. Results of the experimental test bench (dark line) are compared with those of the numerical modeling (gray line).
The frequency range as well as the distance from the source is presented in the real scale.

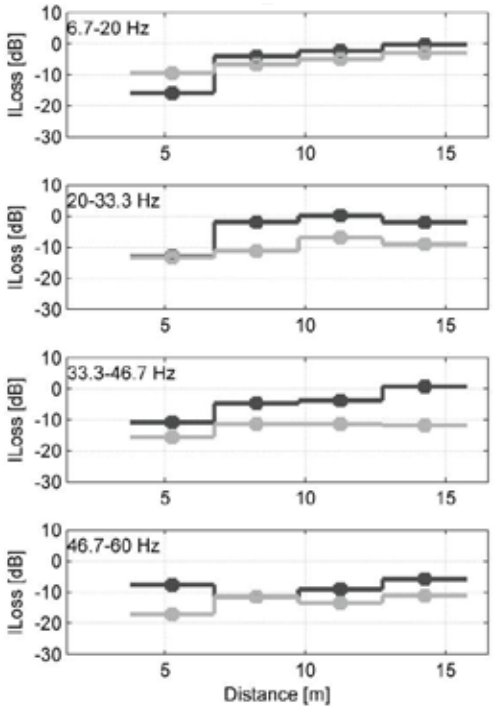

Figure 7. Insertion loss versus distance from the source.

An average insertion loss can also be calculated for each barrier over all distances. A reasonable agreement between the experimental and numerical simulation is observed, figure 8.

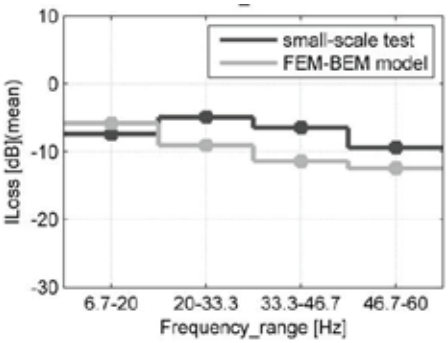

Figure 8. Average insertion loss at different excitation frequencies.

4 CONCLUSIONS

A test bench has been fabricated for the examination of the isolating screen efficiency. Results of the small-scale test show a reasonable agreement with those obtained by the numerical modeling. This confirms the accuracy of the numerical prediction for further investigation.
In addition, results show that the selected concrete screen with a depth of 6 m ($\sim 0.8\lambda$) is not efficient enough to mitigate the vibrations at frequencies lower than 30 Hz. At higher frequencies where H/λ is greater than one, however, higher efficiency has been obtained.

5 ACKNOWLEDGEMENTS

The results presented in this paper have been obtained within the frame of EUROSTAR SOILVIBES project "Railways vibration mitigation in transmission path".
This project is funded by IWT Vlaanderen, the Institute of the Promotion of Innovation by Science and Technology in Flanders. Their financial support is gratefully acknowledged.

6 REFERENCES

Adam M. and von Estorff O. 2005, Reduction of train-induced vibrations by using open and filled trenches. *Computers and Structures*, 83:11–24.

Altaee A. and Fellenius B.H. 1994, Physical modeling in sand. *Canadian geotechnical journal* 31, 420-431.

Celebi E., Firat S., Beyhan G., Cankaya I., Vural I., and Osman K.. 2009, Field experiments on wave propagation and vibration isolation by using wave barriers. *Soil Dynamics and Earthquake Engineering*, 29:824–833.

François S., Schevenels M., Galvin P., Lombaert G., and Degrande G.. 2010, A 2.5D coupled FE-BE methodology for the dynamic interaction between longitudinally invariant structures and a layered half space. *Computer methods in applied mechanics and engineering*, 199(23-24):1536 – 1548.

Garnier J., Gaudin C., Springman S.M., Culligan P.J., .Goodings D, Konig D., Kutter B., Phillips R., Randolph M.F., and Thorel. L. 2007, Catalogue of scaling laws and similitude questions in geotechnical centrifuge modelling. *International Journal of Physical Modelling in geotechnics*, 7(3):1–24.

Miura S. and Toki S. 1982, A sample preparation method and its effect on static and cyclic deformation-strength properties of sand. *Soils and Found.*, 22(1):61–77.

Sieffert J.G. and Cevaer F. 1991, *Handbook of impedance functions, surface foundations*, Ouest editions.

Vaid Y. P., Sivathayalan S., and Stedman D. 1999, Influence of specimen-reconstituting method on the undrained response of sand. *Geotechnical Testing Journal*, 22(3):187–195.